arXiv:hep-ph/9510432v2 31 Oct 1995

CUPP-95/4; TIFR/TH/95-13

September 1995

SINGLET-HIGGS-BOSON SIGNALS AT HADRON COLLIDERS

Anindya Datta [1,♡], *Amitava Raychaudhuri* [1,†], *Sreerup Raychaudhuri* [2,#]

and

Surajit Chakrabarti [3]

[1]Department of Pure Physics, University of Calcutta,

92 Acharya Prafulla Chandra Road, Calcutta 700 009, India.

[2]Theoretical Physics Group, Tata Institute of Fundamental Research,

Homi Bhabha Road, Bombay 400 005, India.

[3]Department of Physics, Maharaja Manindra Chandra College,

20 Ramkanto Bose Street, Calcutta 700 003, India.

ABSTRACT

Many extensions of the Standard Model include $SU(2)_L \times U(1)_Y$ singlet higgs bosons, h^0, and also vectorlike fermions which couple to it. The production and detection possibilities of such singlet neutral scalars at hadron colliders are considered for different scenarios of vectorlike fermions. We find that for some values of masses and couplings, detection at the CERN Large Hadron Collider (LHC) appears to be a distinct possibility, while at the Fermilab Tevatron upgrade the h^0 might be observed only in very favourable circumstances.

Electronic addresses: [♡]anindya@cubmb.ernet.in; [†]amitava@cubmb.ernet.in;

[#]sreerup@theory.tifr.res.in

1 INTRODUCTION

Scalar higgs fields are an important ingredient in the Standard Model (SM) and its popular extensions. Searches for higgs bosons are, therefore, among the important objectives at present and projected colliders. Recent measurements of the ρ parameter (or the oblique T parameter) at the CERN e^+e^- collider LEP-1 yield a result very close to unity [1], which limits the natural possibilities for light scalars to just singlets and doublets of the $SU(2)_L$ component of the SM gauge group. The SM adopts a one-doublet scenario, while extra doublets appear in many of its extensions including the minimal supersymmetric standard model (MSSM) and the left-right symmetric model. Phenomenological consequences of one or more doublets and their detection possibilities have been extensively studied in the literature [2, 3], but the singlet option has not received the same kind of attention. Save for some discussion in the context of Majoron models and non-minimal supersymmetric models [2] one comes across very few studies of singlet higgs bosons.

Interestingly, neutral $SU(2)_L$ singlet scalar particles are predicted in several extensions of the SM. They are present in a natural manner in many Grand Unified Theories (GUTs). For example, the fundamental **27**-plet of E_6, utilised for spontaneous symmetry breaking, includes several such fields [4]. The next to minimal supersymmetric standard model (NMSSM) [5] has just such an extra field to generate the higgs mass parameter – the so-called μ-term. Other models – *e.g.*, the left-right symmetric $SU(2)_L \times SU(2)_R \times U(1)$ model and its GUT extensions like $SO(10)$ [6] – also include singlet scalars. It has also been stressed [7] that in a class of composite models of quarks and leptons such a neutral singlet scalar is an essential

prediction. Moreover, it has been shown [8] that the addition of a singlet higgs scalar (with or without an extra generation of vectorlike fermions) can provide a realistic solution to the fine-tuning problem in the SM. It is therefore of interest to consider strategies for the detection of these scalar singlets (henceforth called singlet higgs bosons) at the present and upcoming colliders.

Barring mixing with the doublet higgs bosons [9], the singlet scalars will not couple to ordinary quarks and leptons. Rather, they will couple to vectorlike fermions – quarks and leptons whose left- and right-handed components transform identically (*i.e.*, both singlets or both doublets) under $SU(2)_L$. Many of the models with singlet higgs bosons include such quarks and leptons. Prominent among these are the E_6 GUT models which contain vector singlet quarks of charge $-\frac{1}{3}$ as well as vector singlet and vector doublet leptons. The composite models of Ref. [7] also contain vectorlike fermions which play an important role in explaining the masses and mixings of the usual quarks and leptons.

The singlet higgs boson could be produced at the CERN e^+e^- collider LEP-1 through the vectorlike fermion loop induced decay $Z^0 \to h^0\gamma$. In an earlier paper [10] two of the authors have considered, with reference to the e^+e^- collider LEP-1, models in which a real singlet higgs boson h^0 occurs together with vectorlike quarks and leptons. Unfortunately, though the signal is relatively clean, the number of such events generally turns out to be too small for effective detection at LEP-1 — even with a catch of $10^7 Z^0$s.

In the present work we analyse possibilities for producing a singlet higgs boson h^0 from gauge boson fusion at hadron colliders. The h^0gg (or $h^0\gamma\gamma$, $h^0Z^0\gamma$, $h^0Z^0Z^0$, $h^0W^+W^-$) interaction will be mediated by a triangle diagram containing vectorlike

quarks (leptons) just as the SM H^0gg interaction is mediated by a top-quark triangle. In fact, as the masses and couplings will be chosen to be rather similar, the numbers produced in the two processes are comparable. Detection of the h^0, however, will require modified strategies since its decay modes are quite different from the SM H^0 and depend on the vectorlike fermion scenario being considered. In general, we find the $h^0 \to \gamma\gamma$ mode to be the most promising one, since the occurrence of hadronically quiet hard photon pairs with a peak in the invariant mass is a clear signal for the decay $h^0 \to \gamma\gamma$. For sufficiently large values of the singlet mass m_h, the $h^0 \to Z^0\gamma \to \ell^+\ell^-\gamma$ and $h^0 \to Z^0Z^0 \to \ell^+\ell^-\ell^+\ell^-$ modes ($\ell = e, \mu$) also become viable. We have estimated SM backgrounds to these processes using a parton-level Monte Carlo event generator and discussed ways of reducing them through appropriate kinematic cuts.

The plan of this article is as follows. In Section 2 we discuss those couplings of the singlet h^0 at tree level and at one-loop level which are relevant for this analysis. We then consider various possible vectorlike fermion scenarios and discuss their relative viability insofar as detection of the h^0 is concerned. In Section 3 we discuss the possible modes of production of the h^0 at hadron colliders. Section 4 is devoted to a study of the decay modes of the h^0 in various scenarios and the possible signals. Backgrounds to these are also analysed in Section 4 and our conclusions are stated in Section 5.

2 COUPLINGS AND GENERAL STRATEGY

As explained above, the neutral singlet scalar h^0 has no $SU(2)_L \times U(1)_Y$ quantum numbers at all and hence does not couple to the SM gauge bosons at tree level. Apart

from quartic interactions of the form $H^\dagger H h^2$ it has no interactions with the standard model quarks, leptons and higgs. However, it can couple to vectorlike singlet or doublet fermions, and the couplings can be written as

$$\begin{aligned} \text{singlet}: \quad \mathcal{L}_s^{hf\bar{f}} &= \bar{f}_s(\xi_s + i\eta_s\gamma_5)f_s h \\ \text{doublet}: \quad \mathcal{L}_d^{hf\bar{f}} &= \bar{f}_d(\xi_d + i\eta_d\gamma_5)f_d h \end{aligned} \tag{1}$$

where the subscripts s, d refer to singlet and doublet respectively and ($\overline{f}_d = [\overline{U}_d, \overline{D}_d]$). The vectorlike fermions couple to the Z^0 boson as

$$\begin{aligned} \text{singlet}: \quad \mathcal{L}_s^{Zf\bar{f}} &= -\frac{g}{\cos\theta_W} Q_f \sin^2\theta_W \overline{f_s}\gamma_\mu f_s Z^\mu \\ \text{doublet}: \quad \mathcal{L}_d^{Zf\bar{f}} &= -\frac{g}{\cos\theta_W}(Q_f \sin^2\theta_W - T_{3f})\overline{f_d}\gamma_\mu f_d Z^\mu \end{aligned} \tag{2}$$

and to photons and gluons through the usual QED and QCD couplings. In the subsequent discussion the symbol f wil be used to denote vectorlike fermions generically. The Yukawa couplings $\xi_{s,d}$ and $\eta_{s,d}$ are arbitrary and we examine the cases $\xi = \eta = 1, \xi = 1, \eta = 0$ and $\xi = 0, \eta = 1$. One notes that the singlet and doublet vectorlike fermions can have gauge-invariant mass terms and hence it is not essential to relate the Yukawa couplings to their masses. One of the results of this is that we have no handle on the mass of the vectorlike fermions except the lower bound $m_f > \frac{1}{2}m_Z$ from the non-observation of the decays $Z^0 \to f\bar{f}$ at LEP-1. It should be noted that we assume *no mixing* between the singlet higgs boson and its standard counterpart and similarly between the vectorlike fermions and their ordinary counterparts. As a result our analysis is not constrained by mass bounds derived using such mixings.

Since the singlet higgs boson does not couple to any of the constituents of the proton, it is clear that it cannot be produced in pp or $p\bar{p}$ collisions through tree-level diagrams. At the one-loop level, however, h^0 can be created via gg (or $\gamma\gamma, Z^0\gamma, Z^0Z^0, W^+W^-$)

fusion through a triangle of vectorlike quarks or leptons as the case may be. The mechanism is illustrated in Fig. 1(a) where V_i, V_j can be any of the pairs of vector bosons mentioned above. Fig. 1(b) exhibits the diagram corresponding to loop-induced decay of the h^0.

To perform a general analysis of the production and decay of the singlet higgs boson we need to know the partial width (Γ) and the branching fractions of processes of the type $h^0 \to V_i V_j$. The fermion in the loop can be any of $f = U_s, D_s, U_d, D_d, L_s, N_d, L_d$, depending on the scenario under consideration, but not N_s. Here U, D refer respectively to quarks of charge $\frac{2}{3}$ and $-\frac{1}{3}$ and L, N to leptons of charge -1 and 0. We can write the transition amplitude for the generic process as

$$\mathcal{M} = \epsilon_\mu^{(i)}(p_i)\epsilon_\nu^{(j)}(p_j)\Gamma_f^{\mu\nu} \tag{3}$$

where the effective coupling $\Gamma_f^{\mu\nu}$ can be written in the schematic form [10]

$$\Gamma_f^{\mu\nu} = \sum \frac{\alpha\omega_{if}\omega_{jf}m_f}{\pi} C_{ij}^f \left[\xi_f(F_1^{ij} g^{\mu\nu} - F_2^{ij} p_j^\mu p_i^\nu) + i\eta_f F_3^{ij}\epsilon^{\mu\nu\rho\delta} p_{i\rho} p_{j\delta}\right]. \tag{4}$$

Here the summation is operative only for the vector doublet fermion scenario and runs over the members of the multiplet. Further, a sum over repeated greek indices is implied. The factors ω_{if}, ω_{jf} depend on the gauge bosons V_i, V_j and the vectorlike fermion scenario under consideration. A list of the possibilities is given in Table 1. The colour factors C_{ij}^f are given in Table 2. The presence of an overall m_f can be explained by helicity flip arguments. The form factors $F_1^{ij}, F_2^{ij}, F_3^{ij}$ are calculated in terms of the well-known two- and three-point functions of 't Hooft and Veltman and Passarino and Veltman [11],

$$F_1^{ij} \;=\; B_0(m_f, m_f; m_h) - 4C_{24} - \frac{1}{2}m_h^2 C_0$$

$$
\begin{aligned}
F_2^{ij} &= 4(C_{23} - C_{22}) - C_0 \\
F_3^{ij} &= -C_0. \qquad (5)
\end{aligned}
$$

where each of the C functions has arguments $C(m_f, m_f, m_f; m_{V_i}, m_{V_j}, m_h)$. If at least one of the gauge bosons V_i, V_j is massless, these can be written in closed form [10, 12], but if both are massive, they have to be expressed in terms of rather complicated formulae involving dilogarithms. These are evaluated using a computer code [13] developed using the algorithms of Ref. [11].

If V_i, V_j are either photons or gluons, gauge invariance demands

$$F_1^{ij} = p_i.p_j F_2^{ij}. \qquad (6)$$

This is explicitly verified by using relations among the B and C functions which obtain when one of the external masses vanish. These relations can be found in Refs. [10, 11].

At this juncture it seems appropriate to discuss the vectorlike fermion scenario(s) considered in this paper and the various search strategies prescribed for each. Rather than include a complete extra generation of vectorlike quarks and leptons, we have chosen to consider the different possibilities one at a time. This has the advantage of simplicity and is theoretically quite legitimate since these extra fermion representations are anomaly-free due to their vectorlike nature. We thus have the following options:

1. a vectorlike doublet of quarks $\overline{f_d} = (\overline{U_d}, \overline{D_d})$;

2. a vectorlike singlet quark $f = U_s$ of charge $\frac{2}{3}$;

3. a vectorlike singlet quark $f = D_s$ of charge $-\frac{1}{3}$;

4. a vectorlike doublet of leptons $\overline{f_d} = (\overline{N_d}, \overline{L_d})$;

5. a vectorlike singlet lepton $f = L_s$ of charge -1;

A sixth possibility, that of a vectorlike singlet neutrino, has been discounted because it does not couple to any of the SM gauge bosons.

Let us consider scenario 1 in more detail. Since vectorlike doublet quarks couple to all the SM gauge bosons, the possibilities in Fig. 1(a) are for V_iV_j to be any of the pairs gg, $\gamma\gamma$, $Z^0\gamma$, Z^0Z^0, W^+W^-. Of all these, the only one worth considering is the gg mode, not only because the h^0gg coupling is the largest, but because of the high gluon luminosity at a hadron collider. The production mechanism would be analogous to that envisaged for the SM higgs boson from gluon-gluon fusion through a top quark triangle [12], and the numbers obtained are, in fact, comparable. Some of the advantage is lost, however, when we look for the detectable signals for the h^0. The dominant decay modes of h^0 will be $h^0 \to gg$ or $h^0 \to \overline{U_d}U_d, \overline{D_d}D_d$ depending on the masses of h^0 and U_d, D_d (doublet fermions have to be more-or-less degenerate, from the bounds arising from the oblique T parameter). In either case, one would see a pair of hadronic jets which would be lost in the large QCD background. Accordingly, we have to turn to the electroweak modes, *viz.* $h^0 \to \gamma\gamma, h^0 \to Z^0\gamma, h^0 \to Z^0Z^0, h^0 \to W^+W^-$. The last possibility, though it has a large branching fraction (see below), will not be considered further in this work because the hadronic decays of the $W^\pm$ pair would be swamped by the QCD background while the leptonic decays would involve missing transverse energy and momentum due to *two* neutrinos, rendering the analysis based on reconstruction of invariant masses impossible. We choose, therefore, to restrict ourselves to the possibilities that V_i', V_j' are γ or Z^0, as the case

may be. Furthermore we assume that the Z^0 is identified by its charged leptonic decay modes $Z^0 \to \mu^+\mu^-, e^+e^-$, (these decay channels contribute 6.6% to the total Z^0 width) generically denoted $Z^0 \to \ell^+\ell^-$ in the subsequent analysis.

Scenarios 2 and 3 are rather similar. However, all electroweak amplitudes in scenario 3 would be suppressed by the charge $-\frac{1}{3}$ of the D_s quark (see Table 1) which makes detection more difficult.

Scenario 4 is interesting since gluonic couplings are disallowed and one has to rely on electroweak production modes, *i.e.* V_i, V_j can be $\gamma\gamma, Z^0\gamma, Z^0Z^0, W^+W^-$. The lesser numbers of h^0s produced are partially compensated by the large branching ratios now available for the $\gamma\gamma, Z^0\gamma, Z^0Z^0$ decay modes. Of course, the tree-level decay $h^0 \to L^+L^-$ will be the dominant one, *if allowed kinematically*. In this case, the heavy lepton $L^\pm$ should behave rather like a muon, except that its track will show little or no curvature. This last circumstance will, however, render measurement of momenta difficult, so this mode may not, after all, be a good option to pin down the h^0. Scenario 5 is almost identical to 4 except that the $h^0 \to W^+W^-$ mode is absent and the couplings are rather different.

Here it might not be irrelevant to compare the total width of this singlet scalar with that of the SM higgs. For the sake of this discussion we consider two values of the vectorlike fermion mass: 50 and 150 GeV. In Table 3, we present the widths of h^0 in the various scenarios for $\xi = \eta = 1$. For comparison, the width of the 'Standard' Model higgs for a hypothetical top quark mass of 50 and 150 GeV are also presented. Note that beyond the $2m_f$ threshold the singlet higgs width is large as a consequence of the tree level decay and the choice $\xi = \eta = 1$.

As noted earlier, the signal for production and decay of an h^0 at a hadron collider

is a pair of vector bosons V_j', V_j', which are either of γ or Z^0, and whose invariant mass shows a sharp peak (below the $m_h = 2m_f$ threshold) at the singlet higgs mass. The principal SM background to each of these processes comes from $q\overline{q}$ annihilation and gluon gluon fusion to a pair of vector bosons V_i', V_j' through a box diagram. (For the $\gamma\gamma$ final state, *bremsstrahlung* is also an important background.) These backgrounds could be quite significant even after imposing various kinematic cuts. The search strategy suggested, therefore, is to plot the invariant mass distribution of the final decay products in suitable bins. Presence, or otherwise, of an h^0 component will be indicated by an excess of events in the particular bin where the peak of the signal lies (this will naturally depend on the mass of the h^0). The subsequent discussions are based on this strategy. For the decay $h^0 \to Z^0\gamma$, since we identify the Z^0 by its decay to $\ell^+\ell^-$, another possible background will be the radiative process $q\overline{q} \to \ell^+\ell^-\gamma$. This last background can, however, be easily dealt with by requiring isolation of the photon from the l^+ and l^- and demanding that the invariant mass of the lepton pair be around m_Z.

3 HADRONIC PRODUCTION OF THE h^0

It has already been mentioned above that the mechanism for producing h^0 in pp or $p\bar{p}$ collisions will depend upon the vectorlike fermions in the loop. So long as these are quarks, the dominant process will be through gg fusion via a vectorlike quark (Q) triangle, the effective h^0gg coupling being given by Eqs. (3) — (6). Using these, we

obtain, at the parton level, the cross section

$$\begin{aligned}\hat{\sigma}(gg \to h^0) &= \frac{\alpha_s^2 m_Q^2}{64\pi}\sqrt{\hat{s}}(\xi_Q^2 \mid F_2^{gg}(\hat{s}) \mid^2 + \eta_Q^2 \mid F_3^{gg}(\hat{s}) \mid^2)\delta(m_h - \sqrt{\hat{s}}) \\ &= \frac{\pi^2}{16\hat{s}}\Gamma(h^0 \to gg)\delta(m_h - \sqrt{\hat{s}}) \end{aligned} \tag{7}$$

where $\sqrt{\hat{s}}$ is the total centre-of-mass energy of the colliding partons and $\Gamma(h^0 \to gg)$ is the decay width of an h^0 to a gg pair. In view of the other uncertainties involved as regards masses and couplings, we have not included QCD corrections – which can be fairly substantial [14] – to this process. To obtain the inclusive hadronic cross section for h^0 production, $\hat{\sigma}(gg \to h^0)$ must be convoluted with the distribution functions $f_{p/g}(x)$ for the gluons. The resulting formula (for scenario 1) is

$$\sigma(pp, p\overline{p} \to h^0 + X) = \frac{\pi^2}{8sm_h}\Gamma(h^0 \to gg)\int_\tau^1 \frac{dx}{x} f_{p/g}(x) f_{p/g}(\frac{\tau}{x}) \tag{8}$$

where $\sqrt{s}$ is the centre-of-mass energy of the colliding hadrons and τ is a dimensionless quantity given by m_h^2/s.

To obtain numerical estimates for the production cross section we have used a parton-level Monte Carlo event generator incorporating the recent structure function parametrisations of Martin, Roberts and Stirling [15]. The resulting estimates for production of h^0 for three different choices of ξ and η are illustrated in Fig. 2 (a), (b) and (c) for a vectorlike doublet of quarks (scenario 1). The solid curves correspond to $\sqrt{s} = 14$ TeV (LHC) and the dashed curves correspond to $\sqrt{s} = 1.8$ TeV (Tevatron). The kink near $m_h = 100$ (400) GeV in each of these curves corresponds to the $m_h = 2m_Q$ threshold for $m_Q = 50$ (200) GeV where the numerical results are not very reliable.

In Fig. 2, for $\sqrt{s} = 14$ TeV, the cross section has been multiplied by a luminosity of $\mathcal{L} = 10^5$ pb^{-1}/year (*i.e.* the so-called high luminosity option at the LHC) while for

$\sqrt{s} = 1.8$ TeV, the corresponding luminosity has been taken to be $\mathcal{L} = 10^3$ pb^{-1}/year *i.e.* for the projected Tevatron*. It may be seen that at the Tevatron*, one could produce over 10^4 h^0s per year for $m_h < 200$ GeV for $m_Q = 50$ GeV; this number drops to 10 when m_h becomes 500 GeV. For $m_Q = 200$ GeV, the number of h^0s produced per year is less than the number obtained with $m_Q = 50$ GeV over the entire mass range of h^0 except when m_h crosses the $2m_Q$ threshold, when the numbers obtained with the two different fermion masses are more or less the same. This is inevitable in view of the fact that the h^0gg coupling falls rapidly with m_Q. It is interesting to note the contrast with the case of the SM H^0gg coupling, which becomes roughly constant for large m_t. This is because the $H^0t\bar{t}$ coupling is proportional to m_t whereas we have taken the $h^0Q\overline{Q}$ coupling to be a constant (see above).

At the LHC, with the high luminosity option, we immediately notice that one could produce over 10^8 h^0s per year for $m_h < 200$ GeV with $m_Q = 50$ GeV. The corresponding numbers for $m_Q = 200$ GeV are about an order of magnitude smaller.

We see from the Figs. 2(a), (b), and (c) that the number of h^0s produced for three different choices of ξ and η do not produce any significantly different result. Also the trend of variation with m_h is more or less the same in the above three cases. Thus in our analysis we shall use $\xi = \eta = 1$ from now on.

The corresponding estimates for scenarios 2 and 3 are obtained in the same way and are smaller than in scenario 1 as there is just one quark – singlet – in the loop. Fig. 2(d) shows the number of h^0s produced for singlet U-type quarks at the LHC and the Tevatron.

The situations for scenarios 4 and 5 are quite different. Since the loop-fermion is now a lepton, there is no h^0gg coupling. Accordingly we should now expect the h^0 to

be produced from the fusion of $\gamma\gamma, \gamma Z^0, Z^0Z^0$ (and in scenario 4 from W^+W^-) pairs emitted from the parent hadrons. Such electroweak production of the h^0 naturally leads to lower cross sections, not only because of the small couplings involved in emission of γ, Z^0 from the parent quarks, but also due to the lower flux of quarks coming from the proton compared with that of gluons at high energies, especially at the LHC. The parton-level cross section for $\gamma\gamma \to h^0$ is easily obtained by multiplying the same for the $gg \to h^0$ case by the factor $(e\omega_{\gamma f}/g_s\omega_{gf})^4$. The values of $\omega_{\gamma f}$ and ω_{gf} are given in Table 1 and are different for the cases 4 and 5. As in the case of two-gluon fusion, in order to obtain the cross section at the hadron level, one must convolute the parton-level cross section with the quark distribution in the proton (or antiproton) as well as the probability for the emission of a photon from a quark. The relevant formulae can be obtained using the well-known effective photon approximation and are given in Ref. [12]. Accordingly, we have

$$\begin{aligned}
&\sigma(pp, p\overline{p} \to h^0 + X) \qquad (9)\\
&= \frac{8\pi^2}{sm_h}\Gamma(h^0 \to \gamma\gamma)\\
&\times \sum_{a,b} \int_\tau^1 dx_1 \int_{\tau/x_1}^1 dx_2 \int_{\tau/x_1x_2}^1 dx_3 \frac{1}{x_1x_2x_3} f_{q_a/\gamma}(x_1) f_{q_b/\gamma}(x_2) f_{p/q_a}(x_3) f_{p/q_b}(\frac{\tau}{x_1x_2x_3})
\end{aligned}$$

where the sum over a, b runs over valence quarks only. When the h^0 is produced from the fusion of the massive vector bosons $W^\pm, Z^0$, the calculation becomes more complicated. The probability of emission of a massive vector boson from a quark depend on its polarisation, and hence one must consider the polarised amplitudes $\mathcal{M}_{\lambda_1\lambda_2}$ rather than the spin-averaged one we have been discussing till now. The

nonvanishing amplitudes are

$$\begin{aligned}
\mathcal{M}_{00} &= \frac{\alpha m_f \omega_{if}\omega_{jf}\xi_f}{\pi m_{V_i} m_{V_j}}\left[\frac{1}{2}(m_h^2 - m_{V_i}^2 - m_{V_j}^2)F_1^{ij} + \frac{1}{4}\lambda(m_h^2, m_{V_i}^2, m_{V_j}^2)F_2^{ij}\right] \\
\mathcal{M}_{+-} &= -\frac{\alpha m_f \omega_{if}\omega_{jf}}{\pi}\left[\xi_f F_1^{ij} - \frac{\eta_f}{2}\sqrt{\lambda(m_h^2, m_{V_i}^2, m_{V_j}^2)}F_3^{ij}\right] \\
\mathcal{M}_{-+} &= -\frac{\alpha m_f \omega_{if}\omega_{jf}}{\pi}\left[\xi_f F_1^{ij} + \frac{\eta_f}{2}\sqrt{\lambda(m_h^2, m_{V_i}^2, m_{V_j}^2)}F_3^{ij}\right] \qquad (10)
\end{aligned}$$

where $\lambda(x,y,z) \equiv x^2+y^2+z^2-2xy-2yz-2zx$ and i,j are either W,W or Z^0,Z^0 or Z^0,γ. The polarisation-dependent probabilities of emission of massive vector-bosons from a parton are calculated in the effective W,Z^0 approximations for $\sqrt{s} \gg m_{W,Z}$ and are given in Ref. [16]. The final formulae are analogous to Eq. (9) but are rather cumbersome and have not been presented explicitly.

Numerical estimates for the electroweak production of h^0s may be obtained from a parton-level Monte Carlo event generator as before, and are presented in Fig. 2(e) for scenario 4. The numbers are rather small and the behaviour with growing m_h more or less mimics that in the case of strong production. At the Tevatron, h_0 can be produced only via photon photon fusion. But at the LHC it can also be produced via Z^0Z^0, W^+W^- or γZ^0 fusion. The sharp peaks in the plots correspond to the thresholds at $m_h = m_Z, 2m_Z, 2m_W$ and as usual at $2m_f$. Observing the smallness of the numbers of h_0 produced, we will not further analyse the signals from this scenario (and scenario 5, which is similar).

4 DETECTION POSSIBILITIES

Once produced, the h^0 will decay to a pair of vector bosons V_i', V_j' through a vectorlike fermion triangle, or, in case it is sufficiently massive, to a pair of vectorlike fermions.

If the vectorlike fermions are quarks (Q), then the dominant decay modes will be $h^0 \to gg$ for $m_h < 2m_Q$ and $h^0 \to Q\overline{Q}$ for $m_h > 2m_Q$. Neither of these decays will be observable, however, because of the large QCD background. We turn, therefore, to the electroweak decay modes.

The branching ratios for the various decay channels are plotted as functions of m_h (for $m_f = 100$ GeV) in Figs. 3(a) and (b) for the vectorlike fermion scenarios 1 and 2 respectively. The convention followed regarding the different curves is:

1. solid: $h^0 \to \gamma\gamma$ mode;
2. solid with dots: $h^0 \to Z^0\gamma$ mode;
3. large dashes: $h^0 \to Z^0Z^0$ mode;
4. dot-dash: $h^0 \to W^+W^-$ mode;
5. small dash: $h^0 \to f\overline{f}$ mode;
6. dots: $h^0 \to gg$ mode.

As one would expect, there is no W^+W^- mode in Fig. 3(b).

It has already been explained that the W^+W^- decay mode in scenario 1, though quite prominent, may not be viable for detection due to the missing energy carried away by two neutrinos, so we shall concentrate on the $\gamma\gamma, Z^0\gamma, Z^0Z^0$ modes only. For scenarios 1 and 2 (and also 3, though this is not shown), when the vectorlike fermion are quarks, these branching ratios are rather small, being of the order of 10^{-3} or less. However, in these three cases, many more h^0s are produced because of the gluonic mode of production, so this disadvantage is more than offset as we shall see presently.

One notes that for singlet fermions, the couplings of γ and Z^0 are proportional to the charge of the fermion, as a result of which (and the favourable kinematics) the $\gamma\gamma$ mode is the dominant one of the three. For vectorlike doublets, however, the Z^0 couples more strongly than the photons, so that modes with a final Z^0 are enhanced above the purely photonic mode. In fact, the Z^0Z^0 mode, though suppressed by a factor of $\frac{1}{2}$ compared with the $Z^0\gamma$ mode because of Bose statistics, still turns out to be dominant because of the presence of a vectorlike neutrino triangle in the doublet case. However, since we consider the detection of the Z^0 through its $\ell^+\ell^-$ decay channel, both signal and background are suppressed by the relevant branching ratio.

Since the mass of the singlet higgs boson h^0 is unknown, it is convenient to divide the possible mass range into four regions, somewhat as is done in the case of the SM higgs boson. These are

1. Very light: $m_h < 50$ GeV;
2. Light: 50 GeV $< m_h < m_Z$;
3. Intermediate mass: $m_Z < m_h < 2m_Z$;
4. Heavy: $m_h > 2m_Z$.

For light and very light singlet higgs bosons, the only viable decay mode is $h^0 \to \gamma\gamma$; for intermediate mass, the decay $h^0 \to Z^0\gamma$ becomes available; while for the heavy case we also have the decay $h^0 \to Z^0Z^0$. Assuming the Z^0 is to be identified by its $\ell^+\ell^-$ decay mode, we accordingly look for either $\gamma\gamma$, or $\ell^+\ell^-\gamma$ or the so-called 'gold plated' signal $\ell^+\ell^-\ell^+\ell^-$ respectively. Throughout the mass range of the h^0 the $h^0 \to \gamma\gamma$ mode remains viable and the role of the other modes is to present further

options which can add to the signal. For high values of m_h, h^0 production itself goes down, as shown in Fig. 2, and it becomes desirable to look for the the singlet higgs in as many channels as possible.

As we have stated earlier, the principal SM background to each of these processes will come from the tree-level process $q\bar{q} \to V_i' V_j'$ and gluon gluon fusion through a box diagram to $V_i' V_j'$. (*Bremsstrahlung* makes an additional important contribution to the two photon background.) We evaluated the tree diagram contribution using a parton-level Monte Carlo event generator and multiplied the numbers by appropriate factors to take the other process(es) into account (see later). In general, for these processes the vector bosons will be produced closer to the beam-pipe and with softer transverse momentum distributions than in the case of the signal, so that kinematic cuts are helpful to reduce the backgrounds. Even with the above cuts, the signal is quite often smaller than the background, decreasing, in fact, as m_h increases because of a fall in the number of h^0s produced. Accordingly, we adopt the strategy suggested in sec. 2, *viz.* we plot the distribution in the invariant mass of the final products $\gamma\gamma$ or $\ell^+\ell^-\gamma$ or $\ell^+\ell^-\ell^+\ell^-$, as the case may be, and look for a peak indicative of the decay of an h^0.

We shall now turn to the results obtained with a parton-level Monte Carlo generator for the above signals and their respective backgrounds. In each case, we present numbers for the Tevatron* and the LHC (high luminosity option) separately, for the different vectorlike fermion scenarios enumerated above. It may be noted at the very outset that we have used the *same* kinematic cuts (see above) for all the vectorlike fermion scenarios considered and also for studies at the Tevatron with $\sqrt{s} = 1.8$ TeV and the LHC with $\sqrt{s} = 14$ TeV. This rather artificial choice is purely for purposes

of comparison and is not suggested as a prescription for a realistic analysis. One can, for example, relax the cut $E_T^\gamma > 25$ GeV on the transverse energy of the final state photons in the case of vectorlike doublet quarks (scenario 1) at LHC with the high luminosity option, and thereby obtain some information about very light singlet higgs bosons. However the analysis presented in this work is meant to be illustrative and some of the results can be improved if we fix upon a particular vectorlike fermion scenario. Results at the Tevatron upgrade and at the low luminosity option of the LHC can be obtained by scaling the signal by a factor of $\frac{1}{10}$ in either case, while the 1σ fluctuations in the background get scaled by $\frac{1}{\sqrt{10}}$. Since the graphs are plotted on a logarithmic scale, these factors simply correspond to vertical shifts of the entire curve(s) and the numbers may be easily read off.

The $h^0 \to \gamma\gamma$ mode: For 50 GeV $< m_h < m_Z$ the only viable decay mode is $h^0 \to \gamma\gamma$. This is also the dominant one of the electroweak modes with *singlet* fermions in the loop for all mass ranges. The signal will be a pair of hard photons produced back-to-back in the h^0 rest frame (but not in the laboratory frame), whose invariant mass, $M_{\gamma\gamma}$ has a sharp peak around $M_{\gamma\gamma} = m_h$. In Fig. 4(a) we have shown, for scenario 1, *i.e.* a doublet of vectorlike quarks, the number of events expected per year as a function of $M_{\gamma\gamma}$ – in bins of 10 GeV – at the LHC with the high luminosity option (see above). The solid, large dashed, small dashed curves represent the expected signal in relevant bin (should the singlet h^0 have a mass which falls in that particular bin) for $m_Q = 50$, 100, 200 GeV respectively. In view of the sharpness of the resonance, the entire signal will lie in the relevant bin [17]. The kinks correspond to the $m_h = 2m_Q$ thresholds. It may be noted that this contribution goes down more or less steadily as the invariant mass increases. This simply reflects the

fall in h^0 production for increasing m_h. In this analysis, we have imposed a cut on the photon pseudo-rapidity $\eta_\gamma < 2.5$. To obtain a viable signal, it usually becomes necessary to impose a further cut $E_T^\gamma > 25$ GeV. This tells us that *very light singlet higgs bosons (of mass $m_h < 50$ GeV) are unlikely to be seen at hadron colliders.*

The histogram shows the square root of the number of events from the SM background deposited in each bin[1] which is a reasonable measure of the 1σ fluctuation. We have multiplied the numbers obtained from the $q\bar{q} \to \gamma\gamma$ Monte Carlo by a factor of 8 [18] to take into account the di-photon production from gluon gluon fusion and the *bremsstrahlung* contribution. It may be pointed out that the background will be suppressed by the fact that the $\bar{q}$ is a sea-quark at the LHC. Since the signal will be seen as a peak in a particular bin over and above the SM background (and its fluctuations), it is clear that the numbers shown in Fig. 4(a) indicate that detection of the singlet h^0 will be viable in the entire range $m_h = 50$ — 400 GeV for $m_Q = 200$ GeV considered in this paper since we will get more than a 5σ peak in the invariant mass distribution of the photons. With the low luminosity option, it may be difficult to probe more than $m_h \simeq 100$ GeV if $m_Q \simeq 50$ GeV, though this limit goes up to about 200 GeV if m_Q is 100 GeV or more.

We have chosen bins of 10 GeV since this appears typical of present experiments [20]. A coarser resolution will not usually affect the signal, but will increase the background and its fluctuations. For example, if the data is collected in bins of 20 GeV, the background will increase by a factor of about 2 and its fluctuations by about 1.4. This will hardly affect numbers in the high luminosity option, but will reduce

[1]This convention will also be followed in figs. 5-7.

the discovery limits for the low luminosity option still further by about 50 GeV in each case.

Fig. 4(b) shows the same curves for scenario 2, *i.e.,* the quark doublet is now replaced by a singlet U-quark. The curves are roughly similar, except for the slightly smaller number of h^0 produced in this case, and the comments made regarding Fig. 4(a) are equally applicable to this case.

Figs. 5(a) and (b) illustrate the same numbers for scenarios 1 and 2 respectively at the Tevatron* with a centre-of-mass energy of 1.8 TeV and a luminosity of 10^3 pb^{-1}. As in the case of Fig. 4, we have displayed results for $m_Q = 50, 100, 200$ GeV (the solid, large dashed and small dashed curves respectively) and a histogram representing the 1σ fluctuation in the background. Since the Tevatron is a $p\bar{p}$ collider, both the q and the $\bar{q}$ can be valence quarks. Hence, there is no suppression of the background as was the case for the LHC. This is unfortunate for the kind of signal we are investigating in this work. As is clear from Fig. 5, one cannot expect a reasonable signal at the Tevatron* very much above 100 GeV for the most promising situation of light vectorlike quarks in the loop ($m_Q = 50$ GeV). For larger values of the quark mass, the situation is much worse and a 1σ effect is just obtained. At the Tevatron with a luminosity of 100 pb^{-1} one can at best obtain a 2σ effect if the masses of both h^0 and the vectorlike fermion are in the vicinity of 50-60 GeV. Electroweak production at this energy is too small to yield even a single h^0 with the design luminosities, so the corresponding graphs in scenarios 4 and 5 have not been shown. It is obvious that data from the Tevatron or Tevatron* are not likely to impose serious constraints on the scenarios being considered in this work, except for the corner of parameter space where the masses of the singlet and the vectorlike fermions are light and their

Yukawa couplings are large.

The $h^0 \to Z^0\gamma$ mode: For $m_h > m_Z$ the h^0 can decay into a $Z^0\gamma$ pair as well as a $\gamma\gamma$ pair. Fixing on the $\ell^+\ell^-$ decay mode of the Z^0, we look for an isolated photon and a pair of leptons with the demand that the total invariant mass $M_{\ell^+\ell^-\gamma}$ of the final state has a sharp peak which would indicate the presence of an h^0 component. To remove the radiative background from $q\bar{q} \to \ell^+\ell^-\gamma$ we also require the invariant mass of the $\ell^+\ell^-$ pair to lie in the vicinity of m_Z.

In Fig. 6(a) we illustrate, as before, the distribution in invariant mass for the final products at the LHC with the high luminosity option, subject to the following kinematic cuts: (a) Transverse energy of the photon is greater than 25 GeV; (b) Transverse momentum of the leptons are each greater than 20 GeV; (c) All decay products have pseudo-rapidity $\eta < 2.5$; (d) The photon is isolated from the lepton, *i.e.* $\theta_{\gamma l} > 15^0$; (e) The invariant mass of the lepton pair lies between 85 to 95 GeV. (f) The angle between the photon and the reconstructed Z^0 is greater than 10^0. (This helps in removing a significant part of the background.)

The signal is rather small in the range $m_h = 90 - 120$ GeV and has not been exhibited here. As regards the background in this decay channel, we examine the $q\overline{q} \to \gamma Z^0 \to \gamma l^+ l^-$ and the radiative process $q\overline{q} \to \gamma l^+ l^-$ using event generators. The latter contribution is essentially eliminated by the 85 GeV $< m_{l^+l^-} <$ 95 GeV cut. To estimate the contribution to the background from gluon-gluon fusion, we multiply the numbers by a factor of 1.3 [21]. For doublet fermions in the loop, the signal is larger than a 5σ fluctuation of the background upto 400 GeV higgs mass with $m_Q = 200$ GeV. With $m_Q = 50$ (100) GeV, the signal is more than the 5σ fluctuation of the background upto $m_h = 170$ (220) GeV.

Fig. 6(b) contains the results for scenario 2 (*i.e.* for singlet U type quark) and the situation is not as promising. Here also we see that for $m_Q = 200$ GeV the signal is above a 2σ to 5σ fluctuation of background when m_h changes from 150 to 400 GeV. For $m_Q = 100$ GeV, below $m_h = 200$ GeV the signal is very large compared to the background but it falls sharply as m_h crosses the $2m_Q$ threshold. For $m_Q = 50$ GeV, the situation is hopeless as the signal is less than 1σ fluctuation of the background for the entire higgs mass range. This seemingly paradoxical result, in view of the propagator effect with increasing m_Q, is easily explained by considering the branching ratios of Fig. 3. The signal drops rapidly beyond $m_h = 2m_Q$ simply because of the opening-up of the $h^0 \to Q\overline{Q}$ channel. If one considers the low luminosity option, the predictions for scenario 1 are rather similar to the predictions for scenario 2 with the high luminosity option. Scenario 2 with the low luminosity option, is, however, no longer detectable.

At the Tevatron the signal remains below a 1σ fluctuation of the background starting from low higgs mass upto higher ones. We do not present these numbers.

The $h^0 \to Z^0 Z^0$ mode: Finally, we consider the possibility that $m_h > 2m_Z$. For this mass range, the $h^0 \to Z^0 Z^0 \to \ell^+\ell^-\ell^+\ell^-$ channel becomes available in addition to the ones considered before. One notes that out of a final state $\ell_1^+\ell_2^-\ell_3^+\ell_4^-$ it is possible to pair the ℓ^+s and ℓ^-s in two ways, *viz.* $\ell_1^+\ell_2^-, \ell_3^+\ell_4^-$ and $\ell_1^+\ell_4^-, \ell_3^+\ell_2^-$. Only one of these sets corresponds to a process with $h^0 \to Z^0 Z^0 \to \ell^+\ell^-\ell^+\ell^-$ and it is for this pairing that the invariant masses of the two $\ell^+\ell^-$ pairs will peak around the Z^0-boson mass. Demanding, therefore, that two of the four possible $\ell^+\ell^-$ pairs that can be formed have invariant masses close to m_Z, one can remove most of the backgrounds except, naturally, those due to $q\overline{q} \to Z^0 Z^0$. Once again we take into account the gluon gluon

fusion to a pair of Z^0s by multiplying the $q\overline{q} \to Z^0 Z^0$ contribution by a factor of 1.3 [21]. One then considers the invariant mass of all four leptons in the final state, more or less as was done in the previous cases. This is a very clear signal and its analogue for the SM H^0 – where it is a tree-level decay – is widely referred to as a 'gold plated' signal. Unfortunately, however, the rather large mass of the h^0 leads to production of smaller numbers in the first place, so that this signal ultimately turns out to be less promising than the previous ones.

For scenario 1, Fig. 7 shows the distribution in invariant mass $M_{\ell^+\ell^-\ell^+\ell^-}$ for the four final-state leptons in the mass range 180 to 500 GeV at the LHC with the high luminosity option. These plots have been obtained with the kinematic cuts: (a) Transverse momentum of each lepton is greater than 20 GeV; (b) All the leptons have pseudo-rapidity $\eta < 2.5$; (c) Two of the four possible $\ell^+\ell^-$ invariant masses lie in the region 85-95 GeV (see above). (d) The angle betweeen the two reconstructed Z^0s is greater than 10^0.

Once again, these cuts are quite adequate to suppress the background. Though the signal itself is small, one may nevertheless find evidence for the singlet higgs in this channel if $m_h < 210$ GeV for $m_Q = 50$ or 100 GeV while for m_Q ($\simeq 200$ GeV) an upper limit of around 400 GeV can be probed. The situation becomes much worse with the low luminosity option when only the range $m_h = 180 - 200$ GeV can yield an acceptable signal, and that too for $m_Q \simeq 50$ GeV only. At the Tevatron upgrade and the Tevatron*, one hardly predicts anything observable except in the narrow band $180 - 185$ GeV, which is not worth investigating in this mode.

From the above discussion, and the illustrative numbers presented, it appears that at the LHC, with high luminosity, there is a good chance that one will see a

signal for the h^0, especially if it appears in conjunction with a doublet of vectorlike quarks. The question that immediately comes to mind is: how can one distinguish it from the SM higgs boson, which has similar decay modes. To answer this, one must recollect the fact that the SM H^0 has a tree-level coupling to $b\overline{b}$ as a result of which its branching ratios to vector boson pairs (except to W^+W^- and Z^0Z^0, which also occur at tree level) are strongly suppressed. Of course, if a tiny signal, compatible with the SM, should be observed, it could equally well be due to an h^0, with the amplitudes suppressed by small values of η_f and ξ_f or large values of m_f. The distinguishing feature will be the absence of tree-level $b\overline{b}, Z^0Z^0$ and W^+W^- decays. Thus, a higgs boson signal through the processes $H^0 \to \gamma\gamma, H^0 \to Z^0\gamma, H^0 \to Z^0Z^0$, but unaccompanied by the other signatures for the SM H^0, could very well be a signal for a singlet h^0.

5 CONCLUSIONS

We have investigated possibilities for the detection of $SU(2)_L \times U(1)_Y$ singlet scalars, at the LHC and the Tevatron. The production and decay modes of these scalars depend on the presence of vectorlike fermions whose left- and right-handed components transform identically under the gauge group. Setting aside the $h^0 \to gg$ decay mode, which is expected to be swamped by QCD backgrounds, the detectable decays are $h^0 \to \gamma\gamma, h^0 \to Z^0\gamma$, and $h^0 \to Z^0Z^0$ where the Z^0 subsequently decays to a pair of electrons or muons. Among these, the first process $h^0 \to \gamma\gamma$ seems to be the most promising. The other two channels can be interesting if the singlet scalar comes in conjunction with a vectorlike doublet of quarks, but not otherwise.

In all the channels that we have examined there is a sharp drop in the signal above the $m_h = 2m_Q$ threshold due to the opening up of the tree-level $h^0 \to Q\overline{Q}$ decay mode. Thus for a vectorlike fermion mass of 50 GeV only a rather limited region of singlet higgs mass can be explored. On the other hand, for $m_Q = 200$ GeV the signal remains above the 5σ fluctuations of the background upto large higgs masses. It is easily seen that for larger m_Q, though the higgs mass threshold is increased, the signal itself is reduced and will not be more than the 5σ fluctuation of the background.

Irrespective of the decay mode, our findings indicate that it is unlikely that an h^0 signal will be seen at the Tevatron. Only with the commissioning of the LHC can we look forward to a potential detection of this particle. A very light singlet h^0 with mass less than 50 GeV will escape even these tests and one will have to look for its signals in processes other than the ones expected at hadron colliders. Similarly, one cannot constrain models in which a singlet higgs boson h^0 (of any mass) couples only to vectorlike leptons.

Acknowledgements

The authors are grateful to Debajyoti Chowdhury for pointing out an important error in a previous draft. They have also profited from discussions with Gautam Bhattacharyya. The authors acknowledge partial financial support from the University Grants Commission, India (AD) as well as the Council for Scientific and Industrial Research and Department of Science and Technology, Government of India (AR). The work of SR is supported by a project (DO NO. SR/SY/P-08/92) of the Department of Science and Technology, Government of India. SC would like to thank the Distributed Information Centre (DIC), Bose Institute, Calcutta, for computational facilities.

References

[1] *Review of Particle Properties*, *Phys. Rev.* **D50**, 1173 (1994).

[2] J.F. Gunion, H.E. Haber, G.L. Kane and S. Dawson, *The Higgs Hunter's Guide*, (Addison-Wesley Publishing Company, 1990). This also contains a comprehensive survey of the literature.

[3] For a detailed study of the detection possibilities of the MSSM higgs at hadron colliders see Z. Kunszt and F. Zwirner, *Nucl. Phys.* **B385**, 3 (1992).

[4] F. Gürsey and P. Sikivie, *Phys. Rev. Lett.* **36**, 775 (1976); *Phys. Rev.* **D16**, 816 (1977); see also T. Rizzo and J.-A. Hewett, *Phys. Rep.* **183**, 193 (1989).

[5] J. Ellis, J.F. Gunion, H.E. Haber, L. Roszkowski and F. Zwirner, *Phys. Rev.* **D39**, 844 (1989).

[6] H. Georgi, *Particles and Fields 1974*, ed. C.E. Carlson (Am. Inst. Phys., N.Y. 1975); H. Fritzsch and P. Minkowski, *Ann. Phys.* **93**, 193 (1975).

[7] J.C. Pati, *Phys. Lett.* **B228**, 228 (1989);
K.S. Babu, J.C. Pati and H. Stremnitzer, *Phys. Rev.* **D51**, 2451 (1995) and references therein.

[8] A. Kundu and S. Raychaudhuri, Tata Institute report TIFR/TH-94/37 (1994) (unpublished).

[9] For the effect of such mixing on the detection of the standard higgs see T. Binoth and J.J. van der Bij, Freiburg report, HEP-PH-9409332 (unpublished).

[10] S. Raychaudhuri and A. Raychaudhuri, *Phys. Rev.* **D44**, 2663 (1991).

[11] G. 't Hooft and M. Veltman, *Nucl. Phys.* **B153**, 365 (1979);
G. Passarino and M. Veltman, *Nucl. Phys.* **B160**, 151 (1979).

[12] V. Barger and R.J.N. Phillips, *Collider Physics*, (Addison-Wesley Publishing Company, 1987).

[13] B. Mukhopadhyaya and A. Raychaudhuri, *Phys. Rev.* **D39**, 280 (1989).

[14] see, for example, M. Spira, A. Djouadi, D. Graudenz and P. Zerwas, DESY Report 94-123 (December 1994) and references therein.

[15] A.D. Martin, R.G. Roberts and W.J. Stirling, *Phys. Rev.* **D50**, 6734 (1994).

[16] S. Dawson, *Nucl. Phys.* **B249**, 42 (1985).

[17] This is true only if $m_h < 2m_Q$. Beyond the threshold, the width of the singlet higgs is large (see Table 3) and our discussion for that region is only approximate. However, this region is not of much interest, in any case, as the signal suffers a severe depletion due to the drop in the branching ratio (see later).

[18] This is rather conservative. For example, for $m_{\gamma\gamma} = 110$ (130) GeV this factor has been estimated to be 3.55 (3.56) for the LHC [19].

[19] CMS Collaboration, G.L. Bayatian *et al.*, Technical Proposal CERN/LHCC 94-38 (December 1994).

[20] CDF collaboration, F. Abe *et al.*, *Phys. Rev. Lett.* **69**, 3439 (1992).

[21] E.W.N. Glover and J.J. van der Bij, *Nucl. Phys.* **B321**, 561 (1989). Following this work, the usual practice [19, 22] is to multiply the contribution from the $q\overline{q} \to \gamma Z^0, \quad Z^0 Z^0$ subprocess by a factor of 1.3 to take into account the $gg \to \gamma Z^0, \quad Z^0 Z^0$ contribution.

[22] ATLAS Collaboration, W.W. Armstrong, *et al.*, Technical Proposal CERN/LHCC/94-43 (December 1994).

Table 1

Scenario	f	$\omega_{\gamma f}$	ω_{Zf}	ω_{gf}	ω_{Wf}
1	quark doublet	$-Q_f$	$-Q_f \tan\theta_W + 2T_{3f}\csc 2\theta_W$	g_s/e	$\csc\theta_W/\sqrt{2}$
2, 3	singlet quark	$-Q_f$	$-Q_f \tan\theta_W$	g_s/e	0
4	lepton doublet	$-Q_f$	$-Q_f \tan\theta_W + 2T_{3f}\csc 2\theta_W$	0	$\csc\theta_W/\sqrt{2}$
5	singlet lepton	$-Q_f$	$-Q_f \tan\theta_W$	0	0

Table 2

Scenario	f	$C_{\gamma\gamma}$	$C_{\gamma Z^0}$	$C_{Z^0Z^0}$	$C_{g_a g_b}$	C_{WW}	C_{ff}
1	quark doublet	3	3	3	$\frac{1}{2}\delta_{ab}$	3	$\sqrt{3}$
2, 3	singlet quark	3	3	3	$\frac{1}{2}\delta_{ab}$	0	$\sqrt{3}$
4	lepton doublet	1	1	1	0	1	1
5	singlet lepton	1	1	1	0	0	1

Table 3

Higgs width in GeV				
	$m_f = 50$ GeV		$m_f = 150$ GeV	
Scenario	$m_h = 100$ GeV	$m_h = 200$ GeV	$m_h = 100$ GeV	$m_h = 200$ GeV
Doublet Quarks	0.2058	72.854	0.0034	0.0357
Singlet U Quark	0.0515	36.289	0.00085	0.0088
Singlet D Quark	0.0513	36.288	0.00084	0.00874
Doublet Leptons	8.97×10^{-5}	24.128	2.126×10^{-6}	9.39×10^{-5}
Singlet Lepton	8.90×10^{-5}	12.063	2.124×10^{-6}	2.91×10^{-5}
'Standard' Model	0.0034	2.897	0.0028	1.511

Table Captions

Table 1 : Overall factors multiplying the production (and decay) matrix element for different scenarios. The symbol f stands for vectorlike fermions generically. Q_f and T_{3f} denote, respectively, the electric charge and the third component of weak isospin of the vectorlike fermion.

Table 2 : Colour factors multiplying the production (and decay) matrix element for different scenarios. The symbol f stands for vectorlike fermions generically. C_{ij} denotes the relevant colour factors for the decay $h^0 \to V_i V_j$ through a vectorlike fermion loop.

Table 3 : The width of a singlet higgs for $m_h = 100$ and 200 GeV in various vectorlike fermion scenarios with $\xi = \eta = 1$. For comparison, the width of a 'Standard' model higgs with a hypothetical top quark of mass 50 and 150 GeV are also shown.

Figure Captions

Fig. 1: Feynman diagram for (a) the hadroproduction of an h^0 and (b) the loop-induced decay of h^0 to a pair of vector bosons.

Fig. 2: h^0 production rate for a doublet of vectorlike quarks with (a) $\eta = 1$, $\xi = 1$, (b) $\eta = 0$, $\xi = 1$, and (c) $\eta = 1$, $\xi = 0$. The rate for a singlet U type vectorlike quark with $\eta = 1$, $\xi = 1$ is shown in (d) while that for a doublet of vectorlike leptons with $\eta = 1$, $\xi = 1$ is presented in (e). Upper lines correspond to $m_f = 50$ GeV, and lower lines correspond to $m_f = 200$ GeV; high luminosity options are taken both for the LHC (solid lines) and the Tevatron* (dashed lines).

Fig. 3: Branching ratios for h^0 decay with (a) a doublet of vectorlike quarks and (b) a singlet vectorlike U quark. The conventions followed for each of these is the following: (*i*) solid: $h^0 \to \gamma\gamma$ mode; (*ii*) solid with dots: $h^0 \to Z^0\gamma$ mode; (*iii*) large dashes: $h^0 \to Z^0Z^0$ mode; (*iv*) dot-dashed: $h^0 \to W^+W^-$ mode; (*v*) small dashes: $h^0 \to f\bar{f}$ mode; (*vi*) dotted: $h^0 \to gg$ mode. We have set $m_f = 100$ GeV throughout.

Fig. 4: $\gamma\gamma$ signal as a function of invariant mass of the final state in bins of 10 GeV with (a) a doublet of vectorlike quarks and (b) a singlet vectorlike U quark, for $m_f = 50, 100, 200$ GeV (solid, large dashed and small dashed curves respectively) at the LHC with the high luminosity option. The histogram shows the square root of the number of events from the SM background in each bin.

Fig. 5: $\gamma\gamma$ signal as a function of invariant mass of the final state in bins of 10 GeV with (a) a doublet of vectorlike quarks and (b) a singlet vectorlike U quark,

for $m_f = 50, 100, 200$ GeV (solid, large dashed and small dashed curves respectively) at the Tevatron*. The histogram shows the square root of the number of events from the SM background in each bin.

Fig. 6: $\ell^+\ell^-\gamma$ signal as a function of invariant mass of the final state in bins of 10 GeV with (a) a doublet of vectorlike quarks and (b) a singlet vectorlike U quark, for $m_f = 50, 100, 200$ GeV (solid, large dashed and small dashed curves respectively) at the LHC. The histogram shows the square root of the number of events from the SM background in each bin.

Fig. 7: $\ell^+\ell^-\ell^+\ell^-$ signal as a function of invariant mass of the final state in bins of 10 GeV with a doublet of vectorlike quarks for $m_f = 50, 100, 200$ GeV (solid, large dashed and small dashed curves respectively) at the LHC with the high luminosity option. The histogram shows the square root of the number of events from the SM background in each bin.

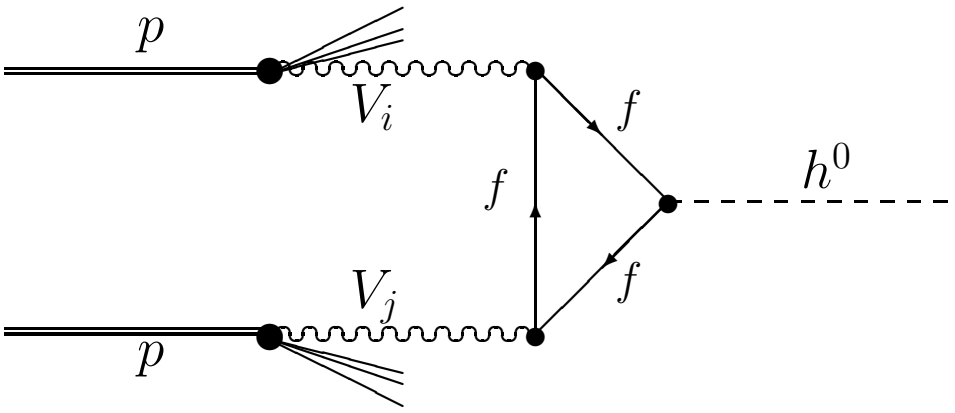

Fig. 1a

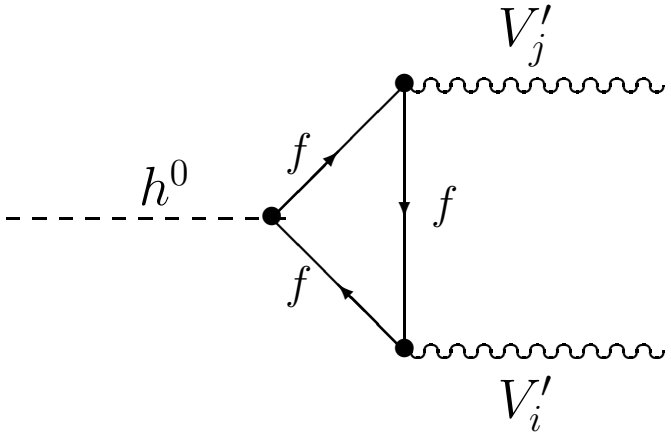

Fig. 1b